Journal of Hazardous Materials, 22 (1989) 283–304
Elsevier Science Publishers B.V., Amsterdam — Printed in The Netherlands

CHEMICAL TRANSPORT IN THE TOP SOIL ZONE — THE ROLE OF MOISTURE AND TEMPERATURE GRADIENTS

YORAM COHEN and PATRICK A. RYAN

Department of Chemical Engineering and National Center for Intermedia Transport Research, University of California, Los Angeles, Los Angeles, CA 90024 (U.S.A.)

(Received January 9, 1989; accepted April 4, 1989)

Summary

The impact of diurnal temperature and moisture profile variations on contaminant transport in the top soil was studied using a one-dimensional transport model. Simulations of the mass transport of benzene, dieldrin and lindane were carried out to illustrate the effect that the diurnal temperature and moisture variations have upon both volatile and slightly volatile species. Model predictions for the volatilization flux of dieldrin, in the absence of convection, varied by at least a factor of 25 between day and night. The results are in qualitative good agreement with experimental data.

1. Introduction

The subject of modeling contaminant volatilization from the soil environment has received considerable theoretical attention in the literature (e.g. Cohen et al. [1]; Freeman and Schroy [2]; Jury et al. [3]; and references therein). These theoretical studies, of pollutant transport in the top soil, have been performed using a variety of model formulations. The simplest soil models describe chemical movement in the air phase and account for chemical adsorption to the soil solid phase. These models assume that an isothermal and uniform moisture description for the top soil is adequate. Such models may also be appropriate for describing long-term unsaturated pollutant transport in nearly dry soils, but they cannot describe the diurnal variations in chemical volatilization rates observed under field conditions (Parmele et al. [4]; Glotfelty et al. [5]). Recently Cohen et al. [1] studied the effects of diurnal field temperature variations on contaminant movement in nearly dry soils, neglecting water movement and moisture gradients. Other recent theoretical studies have focused on the effect of different sorption models in unsaturated soils under isothermal conditions (Corwin [6]), and the effect of both diurnal and seasonal temperature changes [2] on contaminant transport in nearly dry soils. The above models are not appropriate for unsaturated soil conditions where

0304-3894/89/$03.50

liquid water movement and the associated liquid phase dispersion affect liquid phase chemical transport. It is now recognized that in moist soils the rate of chemical diffusion can vary by orders of magnitude [3,1] due to moisture variations in the top soil. In the environment, however, moisture and temperature vary simultaneously, yet none of the existing models have considered the coupled effect of moisture and temperature variations on chemical volatilization in the soil matrix.

The inclusion of diurnal temperature and moisture variations in a chemical transport model is possible by using either a theoretical model (e.g. Schieldge et al. [7]) or field data. Present theoretical models, however, are unable to provide quantitative agreement with measured diurnal temperature and moisture changes at specific soil sites. Therefore, one must rely on field studies in which both temperature and moisture are measured simultaneously. In this paper, the effect of temporal temperature and moisture profiles on dynamic pollutant transport within the soil and across the soil/atmosphere interface are illustrated using a site specific temperature and moisture data set. Model simulations were carried out to illustrate the short term impact (two days to two months) of the temperature and moisture variations on chemical transport processes.

2. Theory

The transport of a contaminant in the multiphase soil matrix consisting of soil-air, soil-water, and soil-solids phases can be described by a set of unsteady convection–diffusion mass balance equations,

$$\frac{\partial(\theta_i C_i)}{\partial t}=\frac{\partial}{\partial z}\left[\frac{\theta_i}{\tau_i} D_i \frac{\partial C_i}{\partial z}\right]-\frac{\partial(\theta_i v_i C_i)}{\partial z}+\frac{\partial}{\partial z}\left[\theta_i D_{vi} \frac{\partial C_i}{\partial z}\right] + R_i+\sum_{j=1}^{3} (Ka)_{ij} (C_j H_{ij}-C_i), \quad i,j=1,2,3, \quad (1)$$

in which C_i is the chemical concentration in phase i moving at an interstitial velocity (cm/s) v_i. The volume content (cm^3/cm^3) of phase i is designated by θ_i, and H_{ij} is the chemical i–j partition coefficient ($H_{ij}=C_i/C_j$). The chemical molecular diffusion and convective dispersion coefficients (cm^2/s) in phase i are D_i and D_{vi}, respectively, and the phase i tortuosity is given by τ_i; R_i is the production or degradation rate for the chemical in soil phase i. Finally, $(Ka)_{ij}$ is the overall phase i volumetric mass transfer coefficient between phases i and j.

Chemical reactions and biological transformations for the chemicals studied in this work (benzene, dieldrin, lindane) were omitted in the simulations, since their time scales are orders of magnitude smaller than the molecular diffusion time scale for the duration of the simulations [8]. From a simple order-of-

magnitude analysis one can show that the presence of the chemical and biological transformations in the chemical transport equations would not produce a discernible change in model predictions. Also, the transport of chemicals by molecular surface diffusion in the solid phase is orders of magnitude smaller than diffusion in the liquid and gas phases, as can easily be verified by noting the much lower surface diffusion coefficients [9]. Thus, solid phase diffusion should have no discernible effect on contaminant migration in the soil and it was therefore neglected in the simulations.

The potential role of water vapor transport on chemical movement is not included in the current model. Water vapor transport may be important when water exists as a discontinuous phase. For the moist soil conditions considered in this work (i.e. where the water phase is assumed to be continuous), however, the water vapor transport effect would not be noticeable except perhaps in the top half centimeter of the soil. It can be shown that chemical transport on the atmosphere-side, however, will dictate the chemical concentration profile on the soil side near the atmosphere/soil interface. Hence, for the conditions of this study the effect of water vapor transport on chemical volatilization was assumed to be negligible.

Finally, given the above simplifications, liquid convection and diffusion in the aqueous and air phases were considered in the following simplified forms of eqn. (1) that describe chemical transport in the air, water, and solid phases of the soil:

Air phase

$$\frac{\partial}{\partial t}(\theta_a C_a) = \frac{\partial}{\partial z}\left[\frac{\theta_a D_a}{\tau_a}\frac{\partial C_a}{\partial z}\right] + (Ka)_{aw}\,(C_w H_{aw} - C_a); \tag{2a}$$

Water phase

$$\frac{\partial}{\partial t}(\theta_w C_w) = \frac{\partial}{\partial z}\left[\frac{\theta_w D_w}{\tau_w}\frac{\partial C_w}{\partial z}\right] - \frac{\partial}{\partial z}(\theta_w v_w C_w) + \theta_w D_{vw}\frac{\partial C_w}{\partial z} + (Ka)_{wa}\,(C_a H_{wa} - C_w) + (Ka)_{ws}\,(C_s H_{ws} - C_w); \tag{2b}$$

Solid phase

$$\frac{\partial}{\partial t}(\theta_s C_s) = (Ka)_{sw}\,(C_w H_{sw} - C_s), \tag{2c}$$

in which the subscripts a, w and s denote the air, water and soil solids phases, respectively. The last term in each of the above equations is the interfacial mass transfer term which provides for the exchange of mass between the air, aqueous, and soil-solid phases. In general, non-linear models of mass exchange between the solid and aqueous phases can be utilized. In the current model, after evaluating available experimental mass transfer data, the simple linear

model was chosen due to its simplicity (see eqn. 2c). The model equations (2a–c) were solved numerically by an implicit finite difference technique subject to the boundary conditions described below.

The bottom boundary condition used in this work was a zero concentration for the chemical at a vertical depth L. The depth L was chosen such that the concentration front had not reached the bottom boundary for the duration of the simulation. It is noted that other boundary conditions could be used, but they would not provide a discernible difference in simulation results for the conditions considered.

The most realistic upper soil boundary condition, at the soil/atmosphere interface, is the flux boundary condition. In general, the atmosphere will be in contact with soil-air, soil-water, and soil-solid phases. Also, the chemical in a soil phase may not be in equilibrium with the adjoining soil phases. Hence, a rigorous flux boundary condition that equates the chemical flux for each separate soil phase present at the soil/atmosphere interface to an equivalent flux on the atmosphere side is more appropriate:

$$\theta_i v_i C_i - \theta_i \left[\frac{D_i}{\tau_i} + D_{vi} \right] \frac{dC_i}{dz} = \alpha_i k_{atm} (C_{atm} - C_i H_{ai}), \quad i=1,2,3 \quad @\ z=0, \tag{3}$$

in which k_{atm} is the atmosphere-side mass transfer coefficient, C_{atm} is the concentration in the atmosphere, and H_{ia} is the given soil phase/atmosphere partition coefficient, and α_i $(0<\alpha_i<1)$ is the normalized area for mass transfer available to phase i on the atmosphere-side. The value of α_i is time-dependent through its dependence on time-dependent variables such as, θ_i, H_{ai}, however, the sum of the normalized areas is constant and equals to unity,

$$\sum_{i=1}^{3} \alpha_i = 1. \tag{4}$$

For the present study involving the three-phase air, water, and soil-solids system, chemical diffusion along the solid phase is assumed to be negligible (hence, $\alpha_s=0$). Consequently, the only contribution to the normalized areas for transfer are from those areas associated with the soil-air/atmosphere and soil-water/atmosphere interfaces. Thus, the corresponding normalized areas are related as follows:

$$\alpha_a = 1 - \alpha_w. \tag{5}$$

For the special case of chemical equilibrium existing between the soil phases, an overall chemical flux from the soil can be obtained by summing eqn. (3) for the air and water phases:

$$\sum_{i=1}^{2} \theta_i v_i C_i - \theta_i \left[\frac{D_i}{\tau_i} + D_{vi} \right] \frac{dC_i}{dz} = k_{atm} (C_{atm} - C_a), \quad @\ z=0, \tag{6}$$

in which knowledge of the α_i are not needed. It is noted that the substitution of eqn. (6) into eqn. (3) results in the following relation for α_i:

$$\alpha_i = \frac{\theta_i v_i C_i - \theta_i \left[\frac{D_i}{\tau_i} + D_{vi}\right] \frac{dC_i}{dz}}{\sum_{i=1}^{N} \left[\theta_i v_i C_i - \theta_i \left[\frac{D_i}{\tau_i} + D_{vi}\right] \frac{dC_i}{dz}\right]}, \quad @\ z=0. \tag{6a}$$

It is worth noting that the value for α_i gives the fraction of the chemical interfacial flux at the soil surface due to phase i. Therefore, the value for α_a as calculated from eqn. (6a) may be considered as a *chemical volatility index*. The value of α_a is unity when chemical transport is through the air phase only, and when α_a is zero chemical transport occurs through the water phase. Hence, the above simplified equation can be used to justify the neglect of either air or liquid phase transport equations in the soil, i.e. neglect of the air phase equation ($\alpha_a \ll 1$) and the water phase chemical transport equation ($\alpha_w \ll 1$). For example, in the absence of convection eqn. (6a) reduces to

$$\alpha_i = \frac{\theta_i (D_i/\tau_i) H_{ia}}{\sum_{i=1}^{N} \theta_i (D_i/\tau_i) H_{ia}}, \tag{6b}$$

where the value of α_i is independent of concentration. For example, the values of α_a, based on eqn. (6b), for benzene, triallate and parathion are listed in Table 1. The results for benzene, which has a relatively low H_{wa}, demonstrate a relatively weak dependence of α_a (relative to triallate and parathion) on the air content. For soil-air contents above 25% by volume the water phase impact on benzene transport is insignificant and transport occurs primarily through the air phase. For triallate and parathion the value of α_a changes from near unity at a volumetric air content of 0.45 to below 0.01 for an air content of 0.05.

TABLE 1

Volatility index[a] for chemicals

Chemical	θ_a	α_a	H_{wa} (20°C)
Benzene	0.45	1.00	5.5
	0.25	0.99	
	0.05	0.63	
Triallate	0.45	1.00	10^3
	0.05	0.009	
Parathion	0.45	0.96	10^5
	0.05	0.00029	

[a]Soil porosity of 0.5 ($=\theta_a+\theta_w$).

This variation in α_a for triallate and parathion demonstrates that the transport pathway for these chemicals is strongly affected by the moisture content of the soil.

When convection of the liquid phase is important the volatility index for the chemical may be calculated from eqn. (6a) once the concentration profiles in the soil-air and soil-water are obtained. The concentration profile in turn must be obtained from the solution of the coupled differential equations (2a–c) with the appropriate boundary conditions. Thus the value of α_i, which is not known *a priori*, in the presence of liquid phase convection must be determined by iteration. As a first guess, the volatility index is approximated by noting that when dispersion coefficients are sufficiently large such that the Péclet number is much smaller then unity, $Pe_w \ll 1 (Pe_w = v_w l/D_{vw})$, the convection terms in eqn. (6a) may be neglected and the equation reduces to

$$\alpha_i = \frac{\theta_i \, (D_i/\tau_i + D_{vi}) \, H_{ia}}{\sum_{i=1}^{N} \theta_i \, (D_i/\tau_i + D_{vi}) \, H_{ia}}. \tag{6c}$$

For each succeeding iteration, the new value for α_i is calculated from eqn. (6a). It is noted that the value for the dispersion coefficient may vary with soil moisture content and fluid phase velocity. Equation (6c) provides a simple approximation for predicting the benchmark characteristics of chemicals in soils. Moreover, the model is attractive due to the small number of input variables, yet general enough to encompass both convective and diffusive processes.

Finally, it is instructive to compare the non-isothermal, non-uniform moisture distribution, and non-equilibrium contaminant transport model, with the commonly employed, isothermal, uniform moisture distribution, equilibrium diffusion model,

$$\frac{\partial C_{soil}}{\partial t} = D \frac{\partial^2 C_{soil}}{\partial z^2}, \tag{7}$$

where D is the effective soil diffusion coefficient which is taken to be independent of space and time. In order to theoretically compare the two models (eqns. 2a–c, 3 to eqn. 7) the effective diffusion coefficient D in eqn. (7) must be appropriately defined. The effective diffusion coefficient D can be defined as the average value over both temperature and moisture fields, as

$$D(t') = \frac{1}{Lt'} \int_0^L \int_0^{t'} D(T, \theta_w) \, dt \, dz, \tag{8}$$

in which t' is the total time elapsed from the beginning of the simulation (i.e. $t=0$) and L is the penetration depth of the concentration front which varies with time. Since, under field conditions, both temperature and moisture vary

with depth and time the effective diffusion coefficient is likely to be "time dependent", and it can only be calculated *after* the solution of the non-equilibrium problem is solved.

3. Simulation set-up

The required model coefficients (in eqns. 2a–c, 3, 5) and their functional dependence on site-specific information and/or chemical properties is shown in Table 2. The two major factors affecting the change in the coefficients listed in Table 2 are temperature and moisture. Therefore, it is necessary to provide a reasonable description of the dynamic temperature and moisture profiles in the soil. Unfortunately, existing theoretical models were not deemed capable of accurately predicting the diurnal temperature and moisture variations. It would be ideal if simultaneous measurements of soil temperature and moisture profiles were available as a function of time in the soil for which contaminant volatilization is being evaluated. Unfortunately, such data are scarce. In fact, to the knowledge of the present authors, the study of Jackson [10] for the Adelanto loam soil is the only one which provides accurate data of simultaneous moisture and temperature profiles. Thus, in this study we have employed the data from the Adelanto loam soil to other similar soils, acknowledging that there may be some differences in the predicted values of the chemical- and soil-dependent transport and partition coefficients. It is our contention, however, that the quantitative effects of moisture and temperature variations are of sufficient accuracy to assess the magnitude of the reported volatilization rates.

The data set of Jackson [10] was obtained for an Adelanto loam soil in Arizona, where simultaneous temperature and moisture data were recorded for soil depths in the range of 0–95 cm at thirty minute intervals for the period of March 3–25, 1971. Prior to data collection, the soil was irrigated beyond ponding. Therefore, in the initial days of data collection the soil was water saturated in the top 2–3 cm. Hence, the initial data represent typical conditions of very high soil-moisture content. At later days the moisture content decreased sig-

TABLE 2

Coefficients in model equations (2a–c) and their functional dependence

Coefficient	Description
$D_a(T)$, $D_w(T)$	molecular diffusion coefficient
$\tau_a(\theta_a)$, $\tau_w(\theta_w)$	tortuosity models
$H_{wa}(T)$	water/air partition coefficient
$H_{ws}(T)$	water/solid partition coefficient
$\lambda(\theta_w)$	dispersion length scale
$v(\theta_w)$	liquid pore-water velocity

nificantly. For example, the volumetric moisture content in the top cm of the soil was determined to have values between 0.03–0.07 on a volume basis for the 14 and 15 March 1971 as compared to values from 39–42.6% (volume of water/volume of soil) for the 3, 4 and 5 March 1971. For purposes of this study, temperature and moisture data, recorded on the 14 and 15 March 1971 (12 days following the initial collection of data), were curve fitted and used in the simulation. These data represent an intermediate stage of soil drying for the site as discussed in the following sections.

3.1. Temperature profile, T

The temperature field data [10] were fitted by the following expressions:

Day 1 (14 March 1971)

$$T = 15.5 - \{15\cos\beta_1 + 4\sin\beta_1\}\exp(-z/8) + \{\cos\beta_2 + 2.7\sin\beta_2\}\exp(-z/8), \quad (9a)$$

Day 2 (15 March 1971)

$$T = 14 - z/64 - 17\cos\beta_1\exp(-z/8) + \{6\cos\beta_2 - 0.6\sin\beta_2\}\exp(-z/8), \quad (9b)$$

in which β_1 and β_2 are defined as:

$$\beta_1 = \pi t/12 - z/10 + \pi/12, \quad (10a)$$

$$\beta_2 = \pi t/6 - z\sqrt{2}/10 + \pi\sqrt{2}/12, \quad (10b)$$

where t is time (hours), z depth (cm) and T the temperature in °C. The exponential terms in eqns. (9a) and (9b) signify the damping of the daily temperature variations with depth. An illustration of the excellent fit of the above correlations to the real time data for day 1 of the simulation is given in Fig. 1.

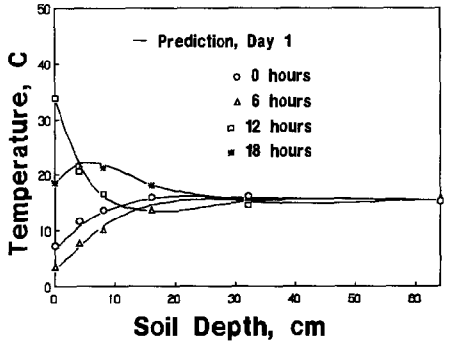

Fig. 1. Comparison of experimental and correlated temperature profiles for 14 March 1971. (Data of Jackson [10].)

3.2 Moisture profile, θ_w

The reported moisture levels near the surface on the 14 and 15 March 1971 [10] are significantly below values initially reported at the field site (3 March 1971); yet, between soil depths of 10 and 75 cm liquid water occupied about 50% of the void space and resulted in significant convection of liquid water. Hence, the data utilized represent an intermediate stage in soil drying. For modeling convenience the moisture data on the 14 and 15 of March 1971 were curve-fitted resulting in the following equations:

Day 1 (14 March 1971)

$$\theta_w = 0.056 + 0.173(1 - e^{-z/2}) - \{0.0098\cos \Omega_1 + 0.0184\sin \Omega_1 + 0.0046[\cos \Omega_2 + \sin \Omega_2]\}e^{-z/2.4}, \quad (11a)$$

for $0 \leq z \leq 7.5$ cm;

$$\theta_w = 0.2096 + 2.26 \times 10^{-3} z - 2.84 \times 10^{-5} z^2, \quad (11b)$$

for $7.5 \leq z \leq 95$ cm;

Day 2 (15 March 1971)

$$\theta_w = 0.0502 + 0.173(1 - e^{-z/2}) - \{0.0112\cos \Omega_1 + 0.0136\sin \Omega_1 + 0.0041\cos \Omega_2 + 0.0136\sin \Omega_2\}e^{-z/2.4}, \quad (12a)$$

for $0 \leq z \leq 7.5$ cm;

$$\theta_w = 0.2067 + 2.10 \times 10^{-3} z - 2.65 \times 10^{-5} z^2, \quad (12b)$$

for $7.5 \leq z \leq 95$ cm;
where Ω_1 and Ω_2 are defined by

$$\Omega_1 = \pi t/12 - z/2.4 + \pi, \quad (13a)$$

$$\Omega_2 = \pi t/6 - z/2.4 + 2\pi, \quad (13b)$$

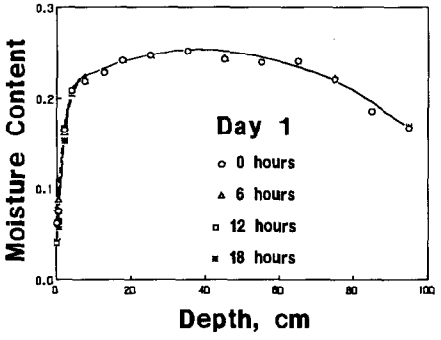

Fig. 2. Comparison of experimental and correlated moisture profiles for 14 March 1971. (Data of Jackson [10].)

where t is time (h) and z is distance from the surface (cm). It is noted that the sine and cosine terms are present to characterize the diurnal cycle of the soil moisture. An example of the fit of the above correlations to the moisture data for four time periods in day 1 are illustrated in Fig. 2. Note that the moisture content at any given depth does not vary significantly with time, but there is a significant moisture gradient near the soil surface.

3.3 Aqueous phase velocity, v_w

The superficial liquid water velocity, v_w (cm/h) was described based on the model of Mualem [11]. The model of Mualem was curve fitted to experimental liquid water velocity data in the Adelanto loam soil. The model was modified in the present work to account for the change in water viscosity with temperature ($(T/T_r)^{7.14}$ factor) to give

$$\theta_w v_w = -7.21\times10^5\left[\theta_w^5\frac{\partial\theta_w}{\partial z}+0.162\left[\frac{\theta_w}{0.426}\right]^{9.5}\right]\times(T/T_r)^{7.14}. \tag{14}$$

It is noted that within the time frame of the simulation, water was moving both up and down the soil column. The upward migration of water occurs within about the top 10 cm of soil. This is due to the combined effects of the mass transfer of soil-water to the atmosphere and capillary forces. Below about 10 cm in the soil the net movement of liquid water is down the soil column due to the dominating effect of gravity.

3.4 Dispersion coefficient, $D_{vw}(c)$

For one-dimensional aqueous phase flow, the dispersion coefficient can be evaluated based on the following model [12]:

$$D_{vw}(c)=\lambda v_w, \tag{15}$$

where λ is a coefficient, often termed the dispersion length scale. A typical field value for λ reported in the literature is 7.81 cm [13]. This dispersion length scale represents the physical characteristic of a nearly saturated agricultural field soil. For unsaturated soils, field data for λ are lacking, but it is noted that laboratory studies show λ to increase as the water content decreases [14–16]. The above findings suggest that it is reasonable to expect that a dispersion length scale of 7.81 cm is too low for unsaturated soil conditions and that λ varies with moisture content. The change in λ with moisture content based on laboratory data for a Glendale loam soil [14,15] can be described by the following empirical relation,

$$\lambda=1.34-1.27\,\theta_w/\theta_w\,(\text{sat}),\ \text{cm} \tag{16a}$$

In order to relate eqn. (16a) to field conditions the above correlation is multiplied by a scaling constant to match λ with the saturated field measurement

of 7.81 cm. The resultant expression for the moisture dependent field dispersion length scale is given by:

$$\lambda = 150\ (1 - 2.225\ \theta_w) \quad \text{for } \theta_w \leq \theta_w(\text{sat}), \tag{16b}$$

where $\theta_w(\text{sat})$ equals to 0.426. By using both the above moisture dependent model for the dispersion length scale and the saturated field measurement value of 7.81 cm, an examination into the sensitivity of chemical transport results as affected by the dispersion length scale can be obtained.

3.5 Molecular Diffusion, D_i

The chemical molecular diffusion in air, D_a, as a function of temperature was estimated, according to Bird et al. [9], by

$$D_a(T) = D_a(T_r)\ (T/T_r)^{1.823}, \tag{17}$$

in which $D_a(T_r)$ is the chemical molecular diffusion coefficient in air at the reference temperature T_r. Similarly, the temperature variation of the chemical molecular diffusivity in water D_w is described by:

$$D_w(T) = D_w(T_r)\ (\mu(T_r)/\mu(T)), \tag{18}$$

where the above model includes the variation in the water viscosity, μ_w, with temperature [9]. The viscosity variation with temperature was determined from a least-squares fit of data provided in the Handbook of Chemistry and Physics [17] for the temperature range of 5 to 40°C, i.e.

$$\mu = \mu(T_r)\ (T/T_r)^{-7.14} \quad T \in [2.78\ \text{K}, 313\ \text{K}]. \tag{19}$$

3.6 Volumetric air/water mass transfer coefficient, $(\text{Ka})_{wa}$

In order to establish whether chemical equilibrium exists between the water and air phases of the soil, the air/water interfacial volumetric mass transfer coefficient must be estimated. Herskowitz and Smith [18] reported that, in general, the different correlations obtained from aqueous/gas phase systems, are in agreement. The model recommended for the liquid-side mass transfer coefficient is given by [19]

$$(ka)_{wa} = 7.8\ D_l\ (\theta_w\ v_w\ \rho_w/\mu_w)^{0.41}\ Sc^{1/2} \tag{20}$$

in which $(ka)_{wa}$ has units of s^{-1}. The Schmidt number is defined as $Sc_w = \mu_l/D_l$, where μ_l is the liquid phase viscosity and D_l (cm^2/s) is the chemical liquid phase molecular diffusion coefficient. For the chemicals considered in this study $Sc_w \gg 1$ and thus $(Ka)_{wa} \simeq (ka)_{wa}$. Finally, ρ_w (g/cm^3) is the density of the liquid phase. It is noted that the above correlation is based on higher liquid velocities and particle diameters (0.54 to 3 mm) than present in most soils. At present, however, no adequate correlations for smaller velocities and particle sizes have

TABLE 3

Atmosphere-side mass transfer coefficient for benzene

Wind speed (m/s)	k_{atm} (cm/s) 20°C
5	32
1	6.5
0.1	0.66

TABLE 4

Physicochemical properties[a] for benzene, dieldrin and lindane at 20°C

Chemical compound	H_{wa} $(C_w/C_a)_{eq}$	H_{sw} $(C_s/C_w)_{eq}$	D_a (cm^2/s)	D_w ($cm^2/s \times 10^{-6}$)	Solubility C_s ($\mu g/ml$)
Benzene	5.5[b]	1.8[d]	0.087	10.2	1780
Dieldrin	2.9×10^3	258[c]	0.043	5.0	0.14[c]
Lindane	1.4×10^4	28[c]	0.058	5.5	8.5[e]

[a]Assumed bulk density of 1.5 g/cm^3.
[b]Leighton and Calo [28].
[c]Jury et al. [3].
[d]Rogers et al. [23].
[e]Mills and Biggar [26].

been reported to the knowledge of the authors, for water/air systems. Thus, in the current work eqn. (20) is adopted acknowledging that some deviations from field conditions are plausible.

3.7 Atmosphere mass transfer coefficient, k_{atm}

The atmosphere-side mass transport coefficient is needed in the boundary conditions given by eqns. (3) and (5). In this study, the mass transfer coefficient k_{atm}, above the soil surface, was calculated based on the relation given by Brustaert [20]. As an example, values of the mass transfer coefficient for benzene, at a few wind speeds above the soil surface, are given in Table 3.

4. Chemical dependent variables

Unfortunately, detailed field data are lacking for volatilization rates, as a function of time. Nonetheless, in order to provide an instructive evaluation of the current modeling approach, the chemicals dieldrin, lindane, and benzene were selected for the simulations (Tables 4 and 5). Dieldrin was selected, since some limited field data exist in the literature for its volatilization flux with time [4]. On the other hand, even though field data are unavailable for lindane, accurate expressions for its partition coefficients as a function of temperature

TABLE 5

Physicochemical properties for benzene, dieldrin and lindane

Chemical compound	Molecular weight	Vapor pressure $\log_{10}$ (mmHg)[c]	Melting temperature, °C
Benzene	78	$15.9 - 2788/(T-50.8)$	5.5
Dieldrin	380.95	$12.07 - 5187/T$[a]	175-176
Lindane	290.8	$13.544 - 5288/T$[b]	113

[a]Spencer and Cliath (1969) $p_s^{(a)}$, [21].
[b]Spencer and Cliath (1983) $p_s^{(s)}$, [22].
[c]Temperature in K.

can be determined based on published data [21,22]. Finally, benzene was selected since its water solubility and Henry's law constant are much higher than either that of dieldrin or lindane.

4.1 Water/solid partition coefficient

The water/solid partition coefficient is equivalent to the product of the water/air and air/solid partition coefficients,

$$H_{ws} = H_{wa} \cdot H_{as}. \tag{21a}$$

Temperature dependent data for the air/solid partition coefficient (i.e. adsorption coefficient) for lindane are available for a Gila silt loam soil [21]. These data were described by the following equation:

$$H_{as} = \exp(-24.5 + 10952/T), \tag{21b}$$

in which T is the temperature in degrees K. Upon substitution of eqn. (21b) into eqn. (21a), the following equivalent expression is obtained for the temperature dependence of lindane water/solid partitioning in the soil:

$$H_{ws} = H_{wa} \exp(-24.5 + 10952/T) \tag{21c}$$

Unfortunately, data on the temperature dependence of benzene and dieldrin partitioning between the solid and aqueous phases of the soil were unavailable. Consequently, for dieldrin the functional form of eqn. (21c) was employed, since lindane and dieldrin are structurally similar; they both have 6 chloride atoms and are ringed molecules. In order to account for differences in the affinity of dieldrin and lindane for adsorption, the temperature dependent lindane adsorption coefficient is multiplied by the ratio of dieldrin to lindane adsorption at 20°C (eqn. 21c), i.e.

$$H_{ws} = H_{ws}(\text{lindane}) \, [H_{ws}(\text{dieldrin})/H_{ws}(\text{lindane})]_{20°C}. \tag{22}$$

For benzene, the temperature dependent model utilized to describe its water/solid partition coefficient is given by [22] as

$$H_{ws} = H_{ws,ref} \exp[-\Delta H_a/R \, (1/T - 1/T_{ref}), \tag{23}$$

where $H_{ws,ref}$ is the benzene water/solid partition coefficient at the tempera-

ture T_{ref} and ΔH_a is the heat of physical adsorption. The value of ΔH_a for benzene was estimated from non-specific adsorption of the aromatic ring on non-polar surfaces [23]. Finally, $H_{ws,ref}$ for benzene was estimated to be equal to 1.8 based on experimental adsorption data for a Hastings soil at 20°C [24].

4.2 Air/water partition coefficient

The temperature dependent air–water partition coefficients for dieldrin and lindane can be estimated based on the simple fugacity approach [25],

$$H_{aw} = M\, p_s^{(s)} / (RT\, C_l^{(s)}) \quad \text{for } T < T_m \tag{24}$$

in which T and T_m are the soil temperature and melting temperature of the compound, respectively. M is the molecular weight of the chemical and R is the universal gas constant, $p_s^{(s)}$ is the chemical saturated solid vapor pressure, and $C_l^{(s)}$ is the liquid solubility of the compound. The variation of the water solubility with temperature for compounds like lindane and dieldrin, which have melting temperatures above the soil temperature, can be calculated from Reid et al. [26],

$$C_l^{(s)} = C_l^{(s)}(T_{ref}) \exp[-\Delta S_f\, T_m\, (T^{-1} - T_{ref}^{-1})/R] \tag{25}$$

where $C_l^{(s)}(T_{ref})$ is the liquid solubility of the solute at the reference temperature; T and T_m are the soil and chemical melting temperatures, respectively. Finally, ΔS_f is the entropy of fusion which is approximately equal to 11.2 cal/mol K for lindane based on its water solubility at 20°C [27] and 30°C [21], and it is set to 13.5 cal/mol K for dieldrin based on the molecular structure theory of Yalkonsky [28].

The benzene air/water partition coefficient is estimated from the empirical correlation of Leighton and Calo [29],

$$H_{aw} = 0.21935 \exp(19.02 - 3964/T)/T, \tag{26}$$

where T refers to the Kelvin temperature scale.

4.3 Solid/water mass transfer coefficient, $(Ka)_{sw}$

Solid/water mass transfer coefficient data are generally taken from adsorption experiments. Since these experiments are usually performed by agitating or mixing the water/solids mixture [29], the mass transfer rates are enhanced relative to what is expected for stationary soils. Thus, available data provide upper limit estimates of the solid/water mass transfer coefficient. The upper limit estimates of the solid/water mass transfer coefficient for lindane in Brookston soil and muck are reported to be 0.3 h^{-1} and 0.01 h^{-1} [30], respectively, and for benzene in Hastings soil 0.03 h^{-1} [24].

5. Results and discussion

The role of the site-specific temperature and moisture profiles on the chemical transport of lindane, dieldrin, and benzene in the top soil was examined in several test cases. These test cases considered the sensitivity of model results to the possible moisture dependence of the dispersion length scale as given by $\lambda = 7.81$ cm and eqn. (16b), the temperature dependence of the solid/water partition coefficient as described by eqns. (21a) for lindane, (22) for dieldrin, and (23) for benzene, in the presence and absence of liquid convection. Also, for comparison, results were obtained for isothermal conditions and for the case of a depth invariant moisture content.

5.1 Lindane and dieldrin volatilization

In the initial test cases the volatilization of lindane and dieldrin from the top soil to the atmosphere was examined. The initial condition was that of a soil uniformly contaminated to a depth of 10 cm. Lindane mass transport between the solid and water phases was based on the adsorption/desorption kinetics for the Brookston soil [30]. For dieldrin, chemical equilibrium between the water and solid phases was assumed due to the lack of adsorption/desorption kinetic data. The results of the above test cases for dispersion length scales of 7.81 cm and as given by eqn. (16b) are displayed in Figs. 3 and 4, for lindane and dieldrin, respectively. The results demonstrate that the dispersion length scale can substantially alter lindane and dieldrin movement in the soil. For the length of the simulations almost 30% more lindane and dieldrin volatilized from the soil for $\lambda(\theta_w)$ compared to the case of $\lambda = 7.81$ cm (see Figs. 3 and 4).

It is expected that in many practical instances, for soils not irrigated or only lightly watered, the soil moisture content would be below the values employed

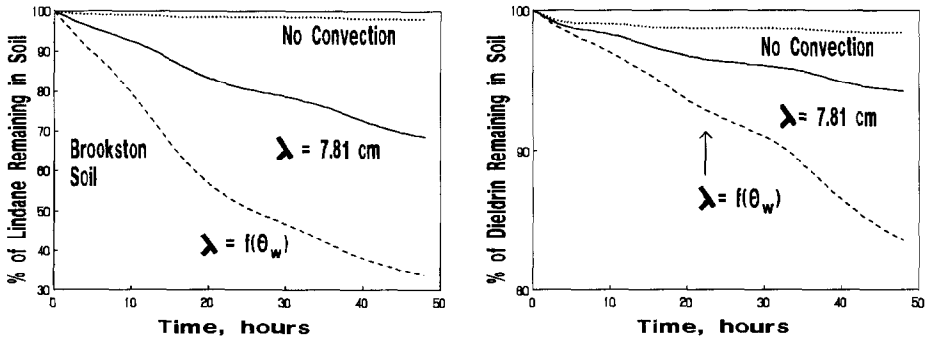

Fig. 3. Simulation of lindane volatilization using Brookston soil adsorption kinetics. Initial contamination depth: top 10 cm.

Fig. 4. Simulation of dieldrin volatilization assuming local chemical equilibrium between the water and solid phase of the soil. Initial contamination depth: top 10 cm.

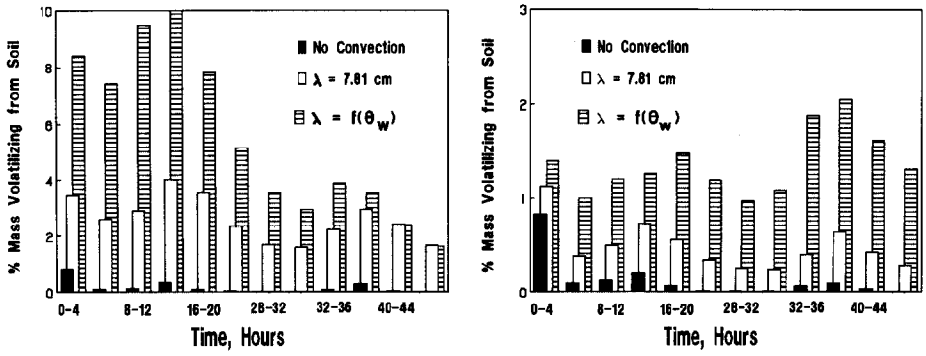

Fig. 5. Percentage of lindane mass volatilization from the soil for consecutive four-hour intervals. Brookston Soil results using Brookston soil adsorption kinetics.

Fig. 6. Percentage of dieldrin mass volatilizing from the soil for consecutive four-hour intervals. Model results assumed local chemical equilibrium between the water and solid phases of the soil.

in the present example, and could be small enough such that the liquid pore velocity would not contribute to chemical transport. Consequently, it is instructive to simulate lindane and dieldrin transport for a liquid pore velocity of zero. This second test case can be considered a limiting example of lindane movement based solely on molecular diffusion. In the absence of convection, the volatilization fluxes of lindane and dieldrin, see Figs. 5 and 6 respectively, are orders of magnitude smaller than their respective volatilization fluxes when convection and dispersion were taken into account. Consequently, for lindane and dieldrin transport in moist soils liquid phase convection dominates all other transport effects.

The increased volatilization rate of lindane and dieldrin in the presence of convection arises due to the effect of the liquid water velocity and dispersion terms in eqn. (2b). Also, for the two values of the dispersion length scale utilized, 7.81 cm and eqn. (16b), a significant difference in the amount of the chemical that volatilizes from the soil was obtained. The above results suggest that in moist soils predicted volatilization rates are very sensitive to the model employed for the dispersion length scale. Thus, realistic predictions for field conditions will require accurate dispersion data to correctly define the functional dependence of the dispersion length scale on moisture content.

The diurnal volatilization rates predicted for lindane and dieldrin are presented in Figs. 5 and 6, respectively, in terms of the percentage of the chemical that volatilizes from the soil in consecutive four hour intervals (of the simulated forty eight hours). All three test cases indicated significant and measurable diurnal variations in the volatilization flux. The volatilization rate was directly correlated with the surface soil temperature; it reached a maximum when the soil temperature was at its highest and a minimum when the soil

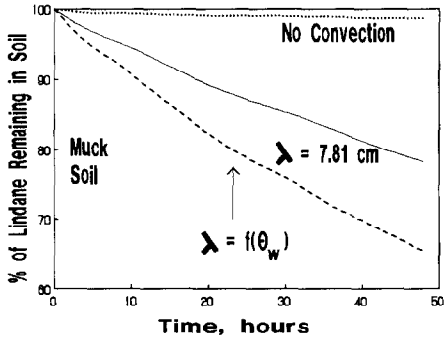

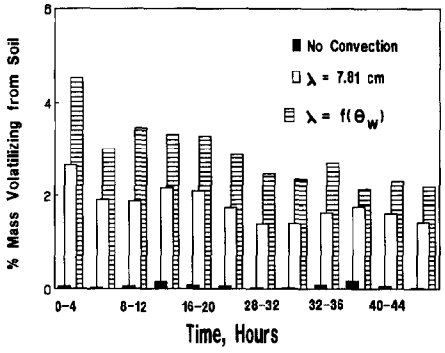

Fig. 7. Simulation of lindane volatilization using muck soil adsorption kinetics. Initial contamination depth: top 10 cm.

Fig. 8. Percentage of lindane mass volatilizing from the soil for consecutive four-hour intervals. Muck soil results use muck soil adsorption kinetics.

temperature was at its lowest. For the test case with no convection, λ equal to 7.81 cm, and as given by eqn. (16b), the maximum-to-minimum volatilization rate ratio of lindane and dieldrin in a diurnal cycle were determined to be 50, 2, 2, and 50, 3, 2, respectively. The above results suggest that when convection is important the diurnal volatilization rate will be small. On the other hand, in the absence of convection the diurnal volatilization rate will vary by a large value between night and day.

It is instructive to compare the above results with the simple diffusion model that assumes an isothermal temperature and a moisture content invariant with depth. The use of a moisture content that is invariant with depth, however, results in negligible water convection. Therefore, it is not surprising that the simple diffusion-model predicted volatilization rates are comparable to the no-convection example and which are over an order of magnitude smaller than the predictions that include temperature and moisture variations.

The set of final test cases for lindane considered adsorption kinetics for muck soil (Fig. 7) [30] and the importance of air/water chemical mass transport. The volatilization of lindane from the soil as affected by muck soil adsorption kinetics show as much as a 100% decrease in the total mass of volatilized lindane compared to results for Brookston soil adsorption kinetics (cf. Figs. 5 and 8). Finally, simulations for the volatilization of lindane, accounting for a finite air/water mass transfer coefficient yielded results which were essentially identical to those based on the assumption of chemical equilibrium between the two phases. Therefore, the assumption of chemical equilibrium between the air and water phases of the soil is reasonable.

5.2 Benzene case studies

The volatilization of benzene from the top soil was also examined based on an initial condition of a uniform soil concentration in the top ten centimeters.

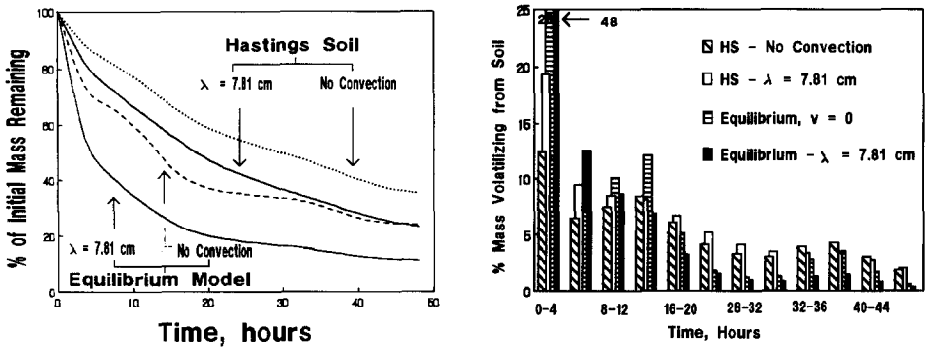

Fig. 9. Simulation of benzene volatilization from the top soil. Equilibrium model assumes local chemical equilibrium between the water and solid phases of the soil. Hastings Soil results use Hastings soil adsorption kinetics. Initial contamination depth: top 10 cm.

Fig. 10. Percentage of benzene mass volatilizing from the soil for consecutive four-hour intervals. Equilibrium model assumes local chemical equilibrium between the water and solid phases of the soil. Hastings Soil results obtained by using Hastings soil adsorption kinetics. Initial contamination depth: top 10 cm. The numbers 28 and 48 in the upper left hand corner of the figure correspond to the percent of benzene mass volatilizing from the soil in the first four hours of the simulation for the case of chemical equilibrium existing between the soil phases with and without water convection, respectively.

The simulations for benzene transport, utilizing the dispersion length scale of 7.81 cm and for the case of no convection are displayed in Fig. 9 (for 48 hours of simulation). These simulations consider benzene volatilization for either the chemical equilibrium assumption between the water and solid phases or using the Hastings soil adsorption kinetics. For the case of chemical equilibrium the benzene mass which remained in the soil after 48 hours for the example of no convection was twice that of the case of convection ($\lambda = 7.81$ cm). A smaller amount of benzene volatilized when adsorption/desorption kinetics were included; after 48 hours, 36% and 23% of the initial benzene mass remained (equivalent to 64% and 77% volatilized mass) for the convection case ($\lambda = 7.81$ cm) and for the case of no convection, respectively. Clearly, the use of adsorption/desorption kinetics compared to the chemical equilibrium assumption may lead to as much as a 100% decrease in the predicted percent of benzene that volatilized in a two day period. It is also apparent that convection increases the rate of chemical volatilization by at least 25% when compared to diffusive transport alone.

It is noted that benzene volatilization rates based on the equilibrium model with convection are similar to the adsorption kinetic-model simulation results without convection (see Figs. 9 and 10). Hence, the effect of convection and adsorption/desorption kinetics on benzene volatilization are comparable. Therefore, it would be difficult to separate the effects of adsorption/desorption

kinetics and convection based solely on field data for benzene volatilization. It is also noted that the diurnal changes in the volatilization rates predicted for the benzene examples are smaller than for the comparable lindane simulations. The simulation results demonstrate that benzene volatilization varies diurnally by at most a factor of two and this occurs in the absence of water convection (see Fig. 10). In conclusion, large diurnal variations in chemical volatilization rates are more apparent for slightly volatile chemicals (i.e. with a relatively large Henry's law constant).

5.3 Dieldrin case study - Comparison to field data

The difficulty in validating contaminant transport soil models stems, in part, from the lack of information gathered in field studies on contaminant volatilization. For example, the lack of an initial condition for the chemical concentration in the soil makes a quantitative comparison between predicted and experimental chemical fluxes impossible. Also, many field studies have focused on chemicals for which the air/water and water/solid partition coefficients are not accurately known.

One study that does provide sufficient, although minimal, information to make a quantitative comparison of measured fluxes to predictions is the dieldrin volatilization study of Parmele et al. [4]. Dieldrin was disced into the soil to a depth of 7.5 cm, assumed uniformly, on the 30 April 1969 [4]. Experimental volatilization fluxes for dieldrin from the soil to the atmosphere were measured on the 30 June 1969. Each volatilization flux measurement was obtained by sampling the air phase for a period of two hours. The data as shown in Fig. 11 exhibit a diurnal variation in the volatilization flux. The maximum volatilization flux was measured during the day (900×10^{-6} ng/cm^2 s) and the minimum flux at night (50×10^{-6} ng/cm^2 s). The ratio of the maximum to minimum measured volatilization flux is 16. In the earlier portion of this paper, it was shown that the predicted diurnal change in the dieldrin volatilization flux in the presence of convection varied by at most a factor of 2. Since the field

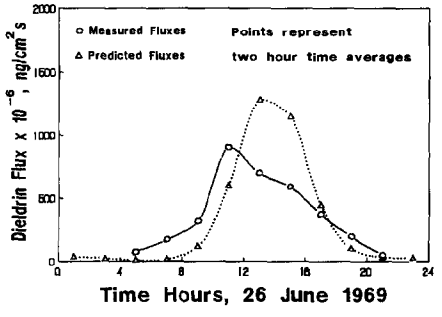

Fig. 11. Comparison of experimental and predicted volatilization rates for dieldrin from the soil to the atmosphere. (Data of Parmele et al. [4].)

data for dieldrin show a maximum change of a factor of 16 in the volatilization flux, during a 24-hour period, it may be inferred that convection was not a major contributor to the dieldrin volatilization fluxes. Consequently, the field data were compared to model predictions in the absence of convection.

Unfortunately, moisture and temperature data were not collected in the Parmele et al. study. Therefore, the moisture and temperature profiles given by eqns. (9a–13b) were utilized in the model predictions. Although one may expect that diurnal temperature variations in the soil for similar regions in the United States will be qualitatively similar, the lack of moisture data for the site, however, negate a quantitative comparison of model predictions to field data. Qualitatively, the theoretical volatilization rates predicted for dieldrin are in good agreement with the field data (cf. Fig. 11) when considering that the exact moisture and temperature profiles for the site were not available. Model results predict the maximum volatilization flux from the soil to be 40% higher than the measured value, and the minimum predicted volatilization flux to be 75% lower than the measured data (at 5 a.m.).

The above qualitative agreement between field data and the diffusion transport model (neglecting convection) suggests that chemical movement in the upper field soil zone is primarily by molecular diffusive transport. The above conclusion is supported by the recent study of Cohen et al. [1] on the long term volatilization of dioxin from nearly dry soils. Liquid convection is important only when chemical soil transport occurs at a moist soil site irrigated to a wetted state (as described in the case studies for lindane and benzene) or for nonvolatile species.

6. Conclusions

A one-dimensional transport model was employed to illustrate the role that dynamic temperature and moisture profiles can have on chemical transport in the top soil zone. The results of the study indicate that for relatively moist soils (where transport of liquid water is possible) the effect of dispersion on chemical volatilization is important. The predicted volatilization flux was found to be a sensitive function of the choice of the dispersion length scale and the adsorption/desorption kinetics.

The application of the current modeling approach to predict the volatilization flux in the environment is presently hampered by the lack of accurate models or field data of simultaneous temperature and moisture profiles. Nonetheless, the current dynamic modeling approach demonstrates the importance of moisture and temperature fluctuations in the presence and absence of liquid water in the soil.

Finally, the results of the current study suggest that the analysis of human health risks, associated with chemical exposure to soil contaminants, should

consider the significant diurnal variability of contaminant volatilization from the soil environment.

Acknowledgements

The authors are grateful to Dr. Ray Jackson (of the United States Department of Agriculture) for providing the diurnal moisture and temperature data obtained from the Adelanto loam soil. This work was partially supported by the United States Environmental Protection Agency Grant CR-812771, and the University of California Toxics Teaching and Training Program.

References

1 Y. Cohen, H. Taghavi and P. Ryan, J. Environ. Qual., 17(2) (1988) 198; Y. Cohen, Environ. Sci. Technol., 20(6) (1986) 538.
2 R.A. Freeman and J.M. Schroy, Environ. Prog., 5(1) (1986) 28.
3 W.A. Jury, W.F. Spencer and W.J. Farmer, J. Environ. Qual., 13(4) (1984) 567, 573, 580; 12(4) (1983) 558.
4 L.H. Parmele, E.R. Lemon and A.W. Taylor, Water Air Soil Poll., 1 (1972) 433.
5 D.E. Glotfelty, A.W. Taylor, B.C. Turner and W.H. Zoller, J. Agric. Food Chem., 32 (1984) 638.
6 D.L. Corwin, J. Environ. Qual., 15(2) (1986) 173.
7 J.P. Schieldge, A.B. Kahle and R.E. Alley, Soil Sci., 133(4) (1982) 197.
8 D.A. Laskowski, C.A. Goring, P.J. McCall and R.L. Swann, Terrestrial environment, in: R. Conway (Ed.), Environmental Risk Analysis for Chemicals. Van Nostrand Reinhold, New York, NY, 1982.
9 R.B. Bird, W.E. Stewart and E.N. Lightfoot, Transport Phenomena. John Wiley & Sons, New York, NY, 1960.
10 R.D. Jackson, Diurnal changes in soil water content during drying, in: R.R. Bruce (Ed.), Field Soil Water Regime. Soil Sci. Soc. Am. Spec. Publ., Vol. 5, 1973; personal communication, 1987.
11 Y. Mualem, Water Resour. Res., 14(2) (1978) 325.
12 Y. Bachmat and J. Bear, Adv. Water Resources, 6 (1983) 169.
13 J.W. Biggar and D.R. Nielsen, Water Resour. Res., 12(1) (1976) 78.
14 M.Th. van Genuchten, P.J. Wierenga and G.A. O'Connor, Soil Sci. Soc. Am. J., 41(2) (1977) 278.
15 M.Th. van Genuchten and P.J. Wierenga, Soil Sci. Soc. Am. J., 41(2) (1977) 272.
16 K.M. Patel and M. Greaves, Chem. Eng. Res. Des., 65 (1987) 12.
17 Handbook of Chemistry and Physics, 61st ed., R.C. Weast (Ed.). CRC Press, Boca Raton, FL, 1980.
18 M. Herskowitz and J.M. Smith, AIChE J., 29(1) (1983) 1.
19 S. Gotto and J.M. Smith, AICHE J., 21 (1975) 706.
20 W. Brustaert, Water Resour. Res., 11(4) (1975) 543.
21 W.F. Spencer and M.M. Cliath, Soil Sci. Soc. Am. Proc., 34 (1970) 574.
22 W.F. Spencer and M.M. Cliath, Residue Rev., 85 (1983) 57.
23 N. Kawabata, I. Higuchi and J. Yoshida, Bull. Chem. Soc. Japan., 54 (1981) 3253.
24 R.D. Rogers, J.C. McFarlane and A.J. Cross, Environ. Sci. Technol., 14(4) (1980) 457.
25 D. Mackay and S. Paterson, Environ. Sci. Technol., 15 (1981) 106.
26 R.C. Reid, J.M. Prausnitz and T.K. Sherwood, The Properties of Gases and Liquids. McGraw-Hill, New York, NY, 1970.

27 A.C. Mills and J.W. Biggar, Soil Sci. Soc. Am. Proc., 33 (1969) 210.
28 S.H. Yalkonsky and S.C. Valvani, J. Chem. Eng. Data, 24 (1979) 127.
29 D.T. Leighton and J.M. Calo, J. Chem. Eng. Data, 26 (1981) 382.
30 B.D. Kay and D.E. Elrick, Soil. Sci., 104(5) (1967) 314.